© 2015. Published by The Company of Biologists Ltd | Journal of Cell Science (2015) 128, 1083–1089 doi:10.1242/jcs.155036

SHORT REPORT

Hypoxia increases the abundance but not the assembly of extracellular fibronectin during epithelial cell transdifferentiation

Manish K. Rana[1,2,‡], Jyoti Srivastava[1,‡,*], Michael Yang[2], Christopher S. Chen[2] and Diane L. Barber[1,§]

ABSTRACT

Increased production and assembly of extracellular matrix proteins during transdifferentiation of epithelial cells to a mesenchymal phenotype contributes to diseases such as renal and pulmonary fibrosis. TGF-β and hypoxia, two cues that initiate injury-induced fibrosis, caused human kidney cells to develop a mesenchymal phenotype, including increased fibronectin expression and secretion. However, upon hypoxia, assembled extracellular fibronectin fibrils were mostly absent, whereas treatment with TGF-β led to abundant fibrils. Fibrillogenesis required cell-generated force and tension. TGF-β, but not hypoxia, increased cell contractility, as determined by phosphorylation of myosin light chain and quantifying force and tension generated by cells plated on engineered elastomeric microposts. Additionally, TGF-β, but not hypoxia, increased the activation of integrins. However, experimentally activating integrins markedly increased the levels of phosphorylated myosin light chain and fibronectin fibril assembly upon hypoxia. Our findings show that deficient integrin activation and subsequent lack of cell contractility are mechanisms that mediate a lack of fibrillogenesis upon hypoxia and they challenge current views on oxygen deprivation being sufficient for fibrosis.

KEY WORDS: Hypoxia, Extracellular matrix, Fibronectin, Fibrosis, TGF-β

INTRODUCTION

Fibrosis, the excessive accumulation of extracellular matrix proteins, is a consequence of sustained tissue injury. Tubulointerstitial fibrosis is a final common pathway in end-stage chronic kidney diseases and is commonly seen with ischemic injury (Zeisberg and Kalluri, 2012; Campanholle et al., 2013; Leung et al., 2013). Fibrosis also occurs in chronic obstructive lung diseases, including asthma, cystic fibrosis and hypertension (Chapman, 2011; Noble et al., 2012). Fibrosis includes increased deposition of the extracellular matrix proteins fibronectin and collagen generated by proliferating resident fibroblasts and also by transdifferentiated epithelial cells that have undergone a fibrosis-associated type 2 epithelial-to-mesenchymal transition (EMT) (Kalluri and Weinberg, 2009; Thiery et al., 2009). An EMT program contributes to hepatic (Teng et al., 2007; Zeisberg et al., 2007), pulmonary (Kim et al., 2006; Chapman, 2011) and renal (Iwano et al., 2002; Liu, 2004; Higgins et al., 2007; Carew et al., 2012) fibrosis, although pericyte fibroblasts also contribute to renal (Lin et al., 2008; Humphreys et al., 2010) and pulmonary (Rock et al., 2011) fibrosis. A better understanding of the cellular responses leading to increased extracellular matrix deposition during EMT could improve therapeutic approaches for limiting fibrosis.

Extracellular cues initiating fibrosis in response to tissue injury include cytokines, such as transforming growth factor β (TGF-β), and hypoxia. Acute and chronic hypoxia promotes pulmonary (Voelkel et al., 2013), renal (Higgins et al., 2007) and hepatic (Nath and Szabo, 2012) fibrosis. However, other than inducing sustained expression of the hypoxia inducible factor HIF1α (Haase, 2009), the molecular and cellular mechanisms whereby hypoxia induces an EMT-like fibrosis remain unresolved. We show that although TGF-β and hypoxia induce an EMT-like transdifferentiation and increase extracellular fibronectin in clonal human HK2 kidney and A549 human lung adenocarcinoma cells, upon hypoxia, assembled extracellular fibronectin fibrils were mostly absent, although there were abundant fibrils upon TGF-β stimulation. Focusing on HK2 cells, which are derived from human adult kidney proximal tubule epithelium, we show that hypoxia is not sufficient to increase fibronectin matrix assembly owing to the lack of integrin activation and sufficient cell contractility to generate fibrils. Our findings provide important new insights on hypoxia-induced epithelial transdifferentiation that impact on current views and possibly therapeutic strategies for treating fibrotic disorders.

RESULTS AND DISCUSSION

Hypoxia increases the abundance, but not assembly, of extracellular fibronectin

We found marked differences in fibronectin deposited by HK2 cells with hypoxia compared with TGF-β. As previously reported (Miettinen et al., 1994; Hocevar et al., 2005; Haynes et al., 2011), incubating HK2 cells with TGF-β (10 ng/ml; 48 h) induced a substantial increase in total cell-associated fibronectin (Fig. 1A), as determined by immunoblotting cell lysates, and in the abundance of extracellular fibronectin (Fig. 1B), as determined by immunolabeling extracellular fibronectin. Hypoxia (1% oxygen) for 48 h also increased the abundance of cell-associated fibronectin compared with normoxia controls (Fig. 1A), in agreement with previous findings (Ryu et al., 2010; Lee et al., 2011), and increased the abundance of extracellular fibronectin (Fig. 1B). However, TGF-β induced a pronounced fibrillar assembly of extracellular fibronectin that was mostly absent upon hypoxia. The hypoxia mimetic dimethyloxaloylglycine (DMOG) also increased extracellular fibronectin but gave limited

[1]Department of Cell and Tissue Biology, University of California, San Francisco, CA 94143, USA. [2]Department of Biomedical Engineering, Boston University and Wyss Institute for Biologically Inspired Engineering, Harvard University, Boston, MA 02215, USA.
*Present address: Novo Nordisk A/S, Vandtaarnsvej 108-110, 2860 Soeborg, Denmark.
‡These authors contributed equally to this work

§Author for correspondence (diane.barber@ucsf.edu)

Received 15 April 2014; Accepted 15 January 2015

Journal of Cell Science (2015) 128, 1083–1089 doi:10.1242/jcs.155036

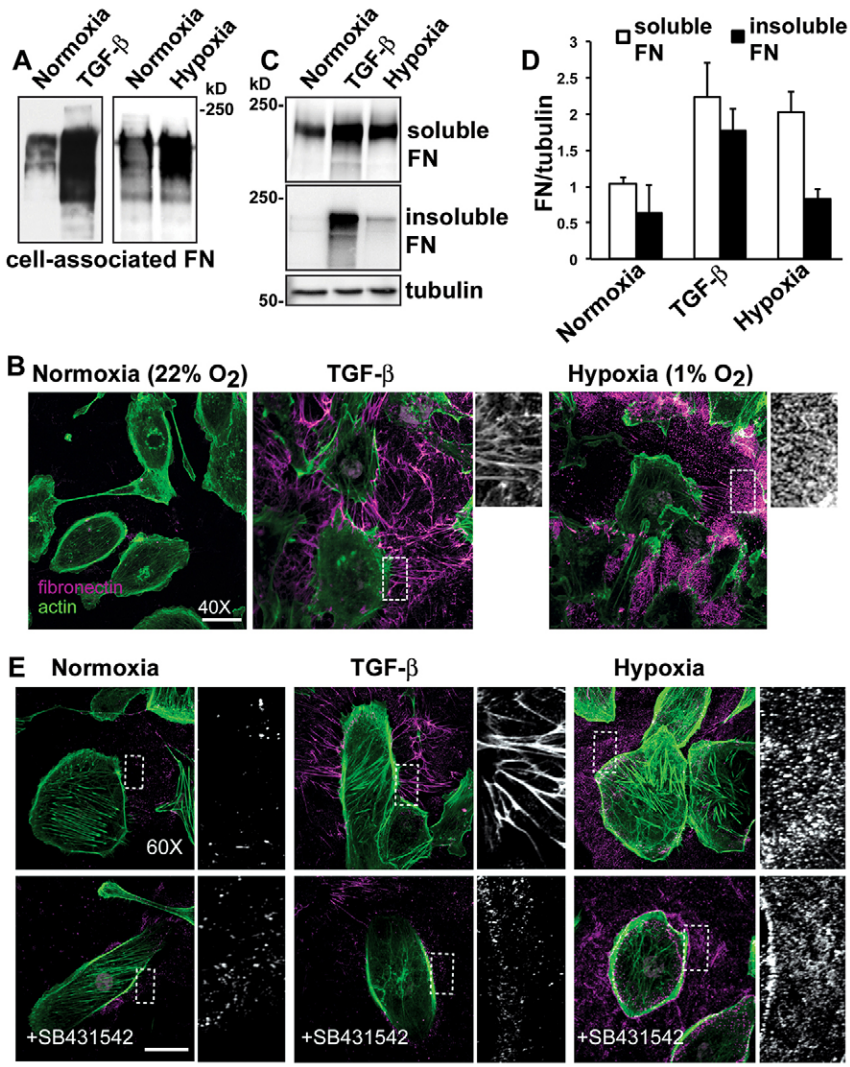

Fig. 1. Hypoxia increases fibronectin abundance but only induces limited fibrillar assembly by HK2 cells. HK2 cells were untreated (normoxia controls), treated with TGF-β (10 ng/ml) in a normoxic environment or maintained at 1% oxygen (hypoxia) and for 48 hours. (A) Immunoblots of cells lysates for fibronectin (FN) under the indicated conditions. (B) Extracellular fibronectin was labeled before cell permeabilization (magenta) and actin filaments were labeled with phalloidin (green) after permeabilization. (C) Immunoblot of cell lysates separated into DOC-soluble and insoluble fractions. Immunoblotting for α-tubulin was used as a loading control. (D) Quantified fibronectin immunoblot signal expressed relative to α-tubulin loading control shown as mean±s.e.m. of three determinations. (E) Immunolabeling, performed as described in B, for extracelluar fibronectin for the indicated conditions in the absence and presence of the TGF-β receptor inhibitor SB431542. Scale bars: 20 μm.

fibril assembly (supplementary material Fig. S1A). We obtained similar results using human lung alveolar A549 cells, which undergo EMT upon exposure to TGF-β (Haynes et al., 2011) and hypoxia (Shin et al., 2012). Although EMT of A549 cells upon hypoxia took 7 days, as indicated by increased fibronectin and actin stress fibers, the fibronectin fibrils seen with TGF-β were mostly absent (supplementary material Fig. S1B). Cell-associated fibronectin is initially soluble in 2% deoxycholate (DOC) but when assembled into mature fibrils is DOC insoluble (McKeown-Longo and Mosher, 1983). For HK2 cells, we confirmed by immunoblotting that a substantial proportion of fibronectin with TGF-β, but not upon hypoxia, was DOC-insoluble (Fig. 1C,D).

We used two approaches to show that responses to hypoxia were independent of TGF-β. First, a luciferase assay performed with mouse lung endothelial cells (MLECs) expressing a truncated PAI-1 promoter that is activated by TGF-β (Abe et al., 1994) revealed that secreted latent and active TGF-β were not different upon hypoxia to those in normoxia controls (supplementary material Fig. S2). Second, blocking TGF-β signaling with SB431542, a pharmacological inhibitor of the TGF-β receptor type 1 (Laping et al., 2002), markedly reduced the increase in assembled fibronectin with recombinant TGF-β but had no effect on increased fibronectin upon hypoxia (Fig. 1E). These findings are in agreement with a previous report showing that hypoxia increases the proximal tubular cell matrix production independently of TGF-β (Orphanides et al., 1997). Hence, hypoxia increases extracellular fibronectin independently of TGF-β receptor activation, and unlike the response to TGF-β, does not substantially increase the assembly of a fibrillar matrix.

Insufficient cell contractility contributes to attenuated fibronectin assembly with hypoxia

The assembly of a fibronectin matrix with TGF-β but not with hypoxia suggested that there are differences in the transdifferentiation process initiated by these two cues. We confirmed both cues increased expression of the transcription factor Snail1 (also known as Snai1) (Fig. 2A,B), an established marker for EMT (Kalluri and Weinberg, 2009), although the abundance of Snail1 upon hypoxia was less than with TGF-β. In transgenic mice, increasing Snail1 in the adult kidney is sufficient to induce renal fibrosis (Boutet et al., 2006). Decreased expression of E-cadherin is also a conserved marker of EMT (Kalluri and Weinberg, 2009; Thiery et al., 2009); however, the low level of E-cadherin expression in undifferentiated HK2 cells prevented us from assessing this marker. N-cadherin, which is expressed in control HK2 cells, increased with TGF-β and

Journal of Cell Science (2015) 128, 1083–1089 doi:10.1242/jcs.155036

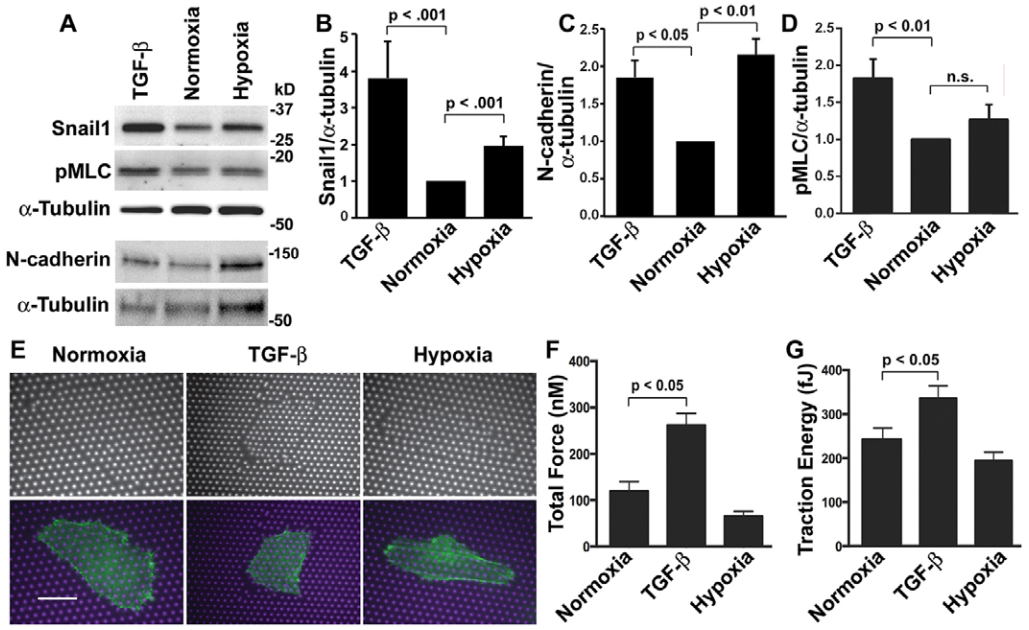

Fig. 2. TGF-β but not hypoxia increases cell contractility. (A) Immunoblots of lysates from normoxia control HK2 cells and cells treated with TGF-β or maintained at 1% oxygen (hypoxia) for 48 h and probed with antibodies for Snail-1, pMLC-Thr18/Ser19 and N-cadherin, and for α-tubulin as a loading control. (B–D) Quantified immunoblot signal for Snail1 (B), N-cadherin (C) and pMLC (D) normalized to the α-tubulin loading control and expressed relative to normoxia controls. Data are mean±s.e.m. of seven independent cell preparations for Snail1, three for N-cadherin and five for pMLC. Statistical differences were determined by the Student's *t*-test. (E) HK2 cells expressing LifeAct–GFP were plated on micromolded PDMS micropost arrays and treated with TGF-β or hypoxia for 48 h. Phase-contrast and fluorescence images are shown in the top and bottom panels, respectively. Merged fluorescence images of microposts (magenta) and cells expressing LifeAct–GFP (green). Scale bar: 15 µm. (F,G) Total force (F) and traction energy (G) quantified from cells plated on microposts. Data are the mean±s.e.m. of >10 cells for each condition in three independent cell preparations.

upon hypoxia (Fig. 2A,C), further confirming transdifferentiation is mediated by both cues. Expression of N-cadherin and the low abundance of E-cadherin suggest that HK2 cells do not have a 'ground state' epithelial phenotype; however increased expression of fibronectin, Snail1 and N-cadherin with TGF-β and upon hypoxia indicate transdifferentiation towards a mesenchymal phenotype.

Transdifferentiation of renal cells increases cell contractility (Fan et al., 2007), and actomyosin contractility is essential for fibrillogenesis to generate mechanical tension that stretches compact soluble fibronectin molecules and unmasks self-association sites for fibril assembly (Leiss et al., 2008; Singh et al., 2010). We found that hypoxia did not increase actomyosin contractility. Immunoblotting cell lysates for phosphorylated myosin light chain (pMLC-Thr18/Ser19; the antibody is specific for phosphorylated MYL2) showed increased abundance with TGF-β but not upon hypoxia compared with normoxia (Fig. 2A,D). We directly measured the contractility of cells plated on micromolded elastomeric microposts that deflect with cell-generated force and tension as described previously (Fu et al., 2010). We used cells expressing LifeAct–GFP, an actin filament reporter (Riedl et al., 2008; Haynes et al., 2011), to identify cells on the fabricated arrays (Fig. 2E). Compared with normoxia controls, TGF-β significantly increased cell contractility, as determined by measuring total force (nN) (Fig. 2F) and traction energy (fJ) (Fig. 2G). In contrast, total force and traction energy upon hypoxia were not significantly different than in normoxia controls (Fig. 2F,G). Hence, although both TGF-β and hypoxia induce transdifferentiation of HK2 cells, cell contractility increases with TGF-β but not upon exposure to hypoxia.

If limited cell contractility is a determinant in attenuated fibrillogenesis upon hypoxia, we predicted that increasing contractility might increase the assembly of deposited fibronectin. We confirmed this prediction by transiently expressing in HK2 cells a mutant expressing phosphomimetic MLC containing aspartic acid substitutions for threonine 18 and serine 19 (MLC-DD), which renders MLC constitutively active and increases cell contractility (Yoneda et al., 2007). MLC wild type (WT) and DD were tagged at the C-terminus with GFP to visualize expression in HK2 cells and extracellular fibronectin was determined by immunolabeling (Fig. 3). Neither MLC construct changed the fibronectin abundance in normoxia controls. Upon hypoxia treatment, there were substantially more fibronectin fibrils with expression of MLC-DD but not MLC-WT (Fig. 3). These findings are in agreement with a previous report showing that fibronectin assembly requires MLC activity (Yoneda et al., 2007), and they indicate that limited cell contractility is at least in part a cause for defective fibrillogenesis upon exposure to hypoxia.

Lack of integrin activation is a mechanism for attenuated fibronectin assembly upon hypoxia

Activation of integrin receptors increases fibrillogenesis and actomyosin contractility (Leiss et al., 2008; Singh et al., 2010) and mediates TGF-β-induced fibrosis (Henderson and Sheppard, 2013). We predicted that lack of integrin activation might be a mechanism for limited cell contractility and fibronectin assembly upon hypoxia. Consistent with this prediction, the abundance of activated β1 integrin relative to total β1 integrin, as determined by immunoblotting, was significantly greater with TGF-β but not hypoxia compared with normoxia controls (Fig. 4A,B). We did

Journal of Cell Science (2015) 128, 1083–1089 doi:10.1242/jcs.155036

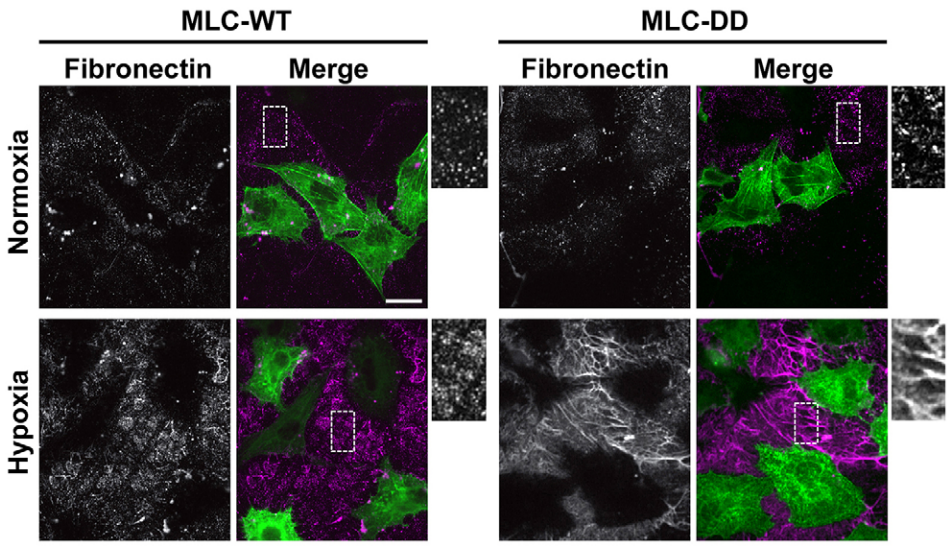

Fig. 3. Phosphomimetic MLC rescues impaired fibrillogenesis with hypoxia. HK2 cells transiently expressing wild-type MLC–GFP (MLC-WT) or MLC-T18D/S19D–GFP (MLC-DD) were untreated (normoxia controls) or exposed to 1% hypoxia for 48 h. Representative images of cells immunolabeled for fibronectin. Scale bar: 20 μm.

find that hypoxia but not TGF-β increased total β1 integrin expression, as previously reported (Cowden Dahl et al., 2005; Keely et al., 2009; Lee et al., 2011). Additionally, both hypoxia and TGF-β increased total α5 integrin expression, as determined by immunoblotting cell lysates (supplementary material Fig. S3A,B), and the abundance of α5 integrin at the cell surface, as determined by fluorescence-activated cell sorting (FACS) (supplementary material Fig. S3C). Hence, the lack of β1 integrin activation upon hypoxia is not due to limited α5β1 expression. Adding $MnCl_2$ (25 μM), which activates integrins (Ni et al., 1998), significantly increased the abundance of activated β1 integrin relative to total β1 integrin as well as the levels of pMLC with normoxia and hypoxia (Fig. 4A–D). Additionally, although hypoxia increased α5 and β1 integrin expression, it did not increase integrin signaling, as indicated by the levels of phosphorylated focal adhesion kinase (FAK, also known as PTK2, denoted pFAK-Y397), which increases with integrin activation. In contrast pFAK-Y397 but not total FAK markedly increased with TGF-β and upon normoxia and hypoxia in the presence of $MnCl_2$ (Fig. 4E,F). Additionally, $MnCl_2$ induced the assembly of extracellular fibronectin fibrils upon normoxia and hypoxia (Fig. 4G), indicating that secreted fibronectin upon hypoxia is assembly competent. These findings reveal that hypoxia-induced epithelial transdifferentiation of HK2 cells leads to insufficient integrin activation, which is a likely determinant for deficient assembly of fibronectin and myosin-based contractility.

Our study shows that although hypoxia induces transdifferentiation of epithelial cells, as indicated by increased abundance of Snail1, N-cadherin and fibronectin, it does not induce a marked assembly of a fibrillar fibronectin matrix like that seen with TGF-β. These findings, which would be difficult to reveal in an animal model, suggest that hypoxia might not be sufficient to induce fibrosis in the absence of other cues such as an inflammatory response, although future studies are necessary to determine the effects of hypoxia on collagen deposition. Our data support a revised view on the role of hypoxia in a fibronectin fibrosis and indicate, as previously suggested (Haase, 2009), that a synergism between hypoxia and TGF-β signaling might be necessary.

MATERIALS AND METHODS

Cell culture

Clonal human HK2 cells (American Type Cell Collection) were maintained in Dulbecco's modified Eagle's medium (DMEM) with Hams F-12 containing 4.5 g/l glucose and supplemented with 10% FBS, 100 U/ml penicillin and 100 mg/ml streptomycin in a humidified incubator at 37℃ in an atmosphere of 5% CO_2 and 95% air (normoxic conditions). For transdifferentiation, HK2 cells were maintained for 48 h in serum- and Ca^{2+}-free keratinocyte medium (Invitrogen) supplemented with 25 mg/ml bovine pituitary extract and 0.2 ng/ml epidermal growth factor. Human lung A549 adenocarcinoma cells (obtained from Harold Chapman, University of California, San Francisco, CA) were maintained in DMEM (4.5 g/l glucose) supplemented with 10% FBS (Invitrogen), 100 U/ml penicillin and 100 μg/ml streptomycin as described previously (Haynes et al., 2011), with transdifferentiation determined in serum-free small airway basal medium (Lonza, Basel, Switzerland). Transdifferentiation was induced by adding recombinant TGF-β (PeproTech, Rocky Hill, NJ) (10 ng/ml for HK2 cells and 5 ng/ml for A549 cells) to the medium of normoxic cells and hypoxia was induced by incubating cells in a humidified modular incubator chamber (HeraCell 240i, Thermo Scientific, Waltham, MA) at 37℃ in an atmosphere of 1% O_2, 5% CO_2 and 94% N_2. Where indicated, the TGF-β receptor inhibitor SB431542 (5 μM; Sigma-Aldrich) was added when initiating transdifferentiation. Also where indicated, HK2 cells were transfected with cDNA encoding GFP-tagged MLC-WT and MLC-DD provided by Atsuko Yoneda, (Tokyo University of Pharmacy and Life Sciences, Japan) by using Lipofectamine 2000 (Invitrogen).

Immunolabeling

For labeling extracellular fibronectin, cells plated on acid-washed glass coverslips were incubated with anti-fibronectin antibodies (Sigma-Aldrich) for 1 h at 37℃, washed in PBS and fixed with 4% formaldehyde for 12 min. Fixed cells were permeabilized with 0.2% Triton X-100 for 5 min, incubated with 3% BSA in PBS for 30 min and then incubated for 1 h with Alexa-Fluor-488- or Alexa-Fluor-568-conjugated secondary antibodies (Invitrogen). Actin filaments were labeled with Rhodamine–phalloidin (Invitrogen) added during secondary antibody incubations. Nuclei were stained with Hoechst 33342

Journal of Cell Science (2015) 128, 1083–1089 doi:10.1242/jcs.155036

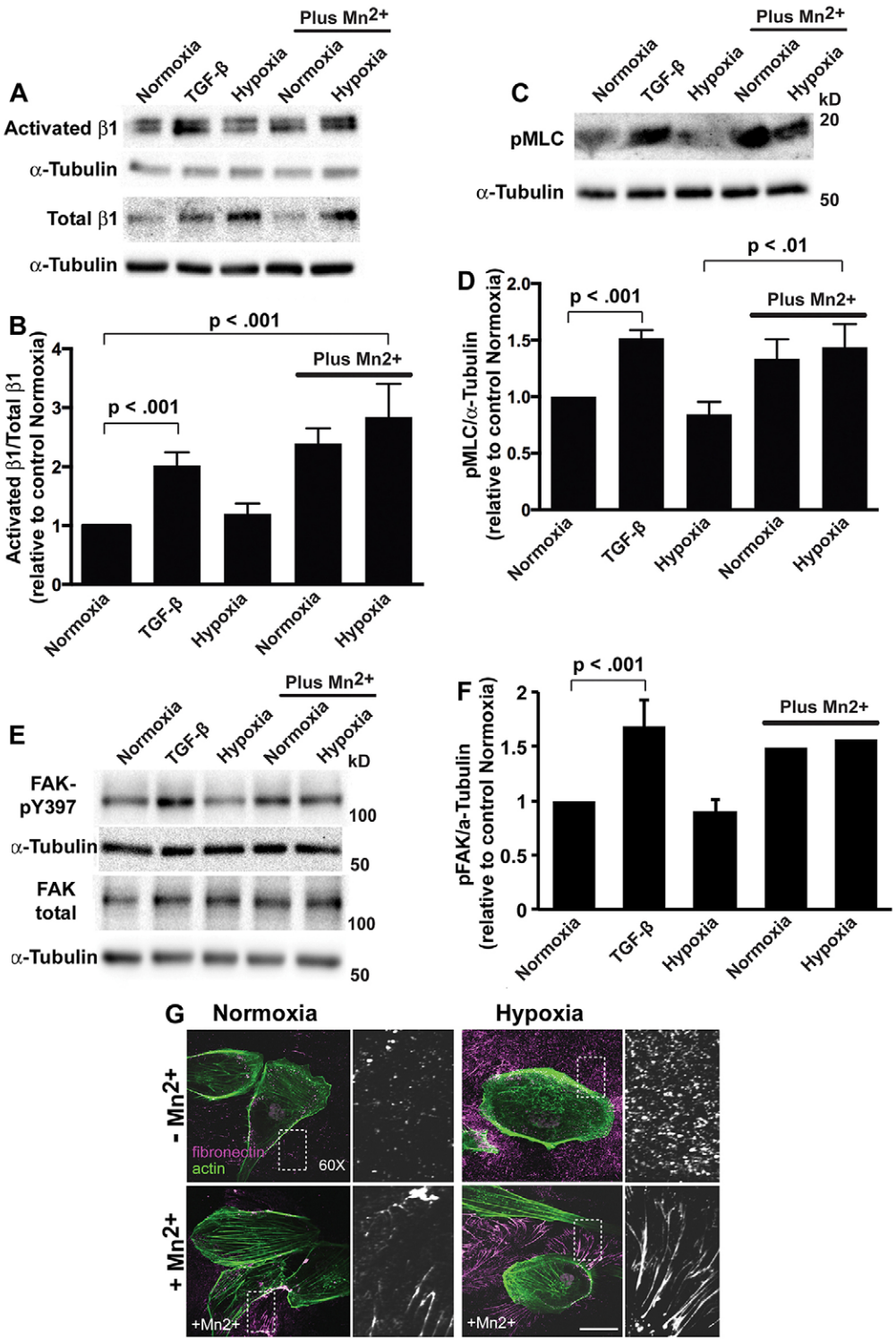

Fig. 4. Activating integrins increases pMLC and fibrillogenesis with hypoxia. (A) Immunoblots for activated and total β1 integrin in lysates from HK2 cells treated for 48 h with TGF-β, exposed to hypoxia or, as indicated, in the presence of 25 μM $MnCl_2$. (B) Quantification of the β1 integrin signals normalized to α-tubulin, calculated as the ratio of activated to total β1-integrin and expressed relative to normoxia controls in the absence of $MnCl_2$. Data are mean±s.e.m. of five independent cell preparations. (C) Immunoblots for pMLC-Thr18/Ser19 (pMLC) in lysates from HK2 cells treated for 48 h with TGF-β, exposed to hypoxia or, as indicated, in the presence of 25 μM $MnCl_2$. (D) Quantified pMLC signal normalized to α-tubulin and expressed relative to normoxia controls in the absence of $MnCl_2$. Data are mean±s.e.m. of three independent cell preparations. (E) Immunoblots for pFAK-Y397 and total FAK in lysates from HK2 cells treated as indicated and described in A and C. (F) Quantified pFAK signal normalized to α-tubulin and expressed relative to normoxia controls in the absence of $MnCl_2$. Data are mean±s.e.m. of three determinations for normoxia, TGF-β and hypoxia in the absence of $MnCl_2$ and averages of two determinations for normoxia and hypoxia with 25 μM $MnCl_2$. (G) HK2 cells with normoxia (controls) and upon hypoxia maintained in the absence or presence of 25 μM $MnCl_2$ for 48 h. Cells were labeled with antibodies for fibronectin (magenta) and stained for actin filaments with rhodamine (green). A magnified view on the boxed area is shown on the right. Scale bar: 20 μm.

(Invitrogen) added to the final wash. Cells were imaged using a 63˚ Plan-Apochromat 1.40 NA or a 40˚ EC Plan-Neofluar 1.30 NA oil immersion objective on a laser-scanning confocal microscope (Zeiss LSM510 META) or a spinning-disk confocal microscopy using a 40× Plan-fluor ELWD 0.6 NA air objective (phase contrast) or a 60× Plan Apochromat TIRF 1.45 NA oil immersion objective on an inverted microscope system (Nikon Eclipse TE2000 Perfect Focus System; Nikon Instruments, Melville, NY) equipped with a spinning-disk confocal scanner unit (CSU10; Yokogawa, Newnan, GA), a 488-nm solid-state laser (LMM5; Spectral Applied Research), a multipoint stage (MS-2000; Applied Scientific Instruments), a CoolSnap HQ2 cooled charge-coupled camera (Photometrics,) and camera-triggered electronic shutters controlled with NIS-Elements Imaging Software (Nikon). Images were processed using NIS-Elements.

Immunoblotting

Proteins in cell lysates obtained in a RIPA buffer were resolved by SDS-PAGE and transferred onto PVDF membranes (Millipore, Haywood, CA)

as previously described (Haynes et al., 2011). Activated β1 integrin was determined using samples prepared and resolved under non-reducing conditions as previously described (Du et al., 2011). Membranes were blocked with 5% non-fat milk or 5% BSA and incubated with primary antibodies for 1 h at room temperature. Primary antibodies included fibronectin and α-tubulin (Sigma-Aldrich), Snail-1 and pMLC-Thr18/Ser19 (Cell Signaling Technologies), FAK (BD Transduction Labs), pFAK-Y397 (Invitrogen), β1-integrin (12G10; Abcam), activated β1 integrin (HUTS-4; Millipore) and α5 integrin (Cell Signaling). After washing, membranes were incubated with horseradish peroxidase (HRP)-conjugated secondary antibodies (Jackson ImmunoResearch Laboratories) for 1 h at room temperature and immunoreactivity visualized with enhanced femto chemiluminescence (Thermo Scientific) and imaged using a BioRad Chemidoc XRS. BioRad Chemidoc XRS Image Lab software was used for semi-quantitative densitometric analysis of immunoblots. Immunoblotting DOC-soluble and -insoluble fibronectin was performed as described previously (McKeown-Longo and Mosher, 1983) using cells lysed in buffer containing 20 mM Tris-HCl pH 8, 2 mM EDTA, 2 mM iodoacetic acid, 2 mM N-ethylaleimide and 2% DOC. Lysates were centrifuged at 20,000 ***g*** for 20 min at 4℃. The DOC-insoluble pellet was resuspended in DOC buffer containing 1% SDS. Proteins in the pellet and DOC-soluble supernatant were separated by SDS-PAGE and probed with anti-fibronectin antibodies.

Luciferase assays

The abundance of secreted TGF-β was determined using MLECs stably expressing a truncated promoter of PAI-1 fused to the firefly luciferase reporter gene as described previously (Abe et al., 1994; Karydis et al., 2009). Conditioned medium collected from normoxic and hypoxic cells was applied to MLECs, for determining active TGF-β, or was heated at 80℃ for 10 min before applying, for determining secreted latent TGF-β. After 24 h MLEC extracts were assayed for luciferase activity using the Luciferase assay system (Promega, Madison, WI) according to the manufacturer's instructions, and luminescence was measured using a Spectramax M5 (Molecular Devices, Sunnyvale, CA) and expressed as relative luciferase units (RLU).

Measurement of cell contractility

HK2 cells stably expressing LifeAct–GFP were plated on micromolded PDMS micropost arrays (Fu et al., 2010) and cells were left untreated (normoxia controls), treated with TGF-β or subjected to hypoxia for 48 h. Cells were imaged at 37℃ using a 60× Plan Apochromat TIRF 1.45 NA oil immersion objective (for fluorescence) on a Nikon spinning-disk confocal microscope, as described for immunolabeling, enclosed in an environmental chamber maintained at 37℃ with 5% CO_2. Images of the Δ9-DiI-stained (red channel) PDMS microposts were acquired at two different focal planes, at the top with the focal plane passing through the top surfaces of the microposts and at the bottom ∼1 µm above the base of the microposts. The two images were analyzed with a custom-developed Matlab program to calculate traction forces (Fu et al., 2010; Yang et al., 2011).

FACS

Trypsinized cells were washed twice (PBS, 2% FBS, 0.1 azide) with centrifugation, resuspended at a concentration of 10^6 cells/ml in PBS with 2% FBS containing anti-α5-integrin antibodies (1 µg/ml; MAB1956Z clone P1D6, Millipore), transferred to polypropylene FACS tubes and incubated on ice for 30 min. Cells were washed by pelleting, resuspended in 1 ml of PBS with 3% BSA containing goat anti-mouse-IgG antibody conjugated to Alexa Fluor 488, incubated for 30 min on ice, washed, and fixed with 1% paraformaldehyde for 15 min. After washing (PBS with 3% FBS), cell pellets were resuspended in 0.5 ml of PBS with 3% BSA and used for FACS analysis to determine levels of cell surface α5 integrin.

Acknowledgements

We thank members of the Barber and Tosten Wittmann laboratories for valuable discussions and Emin Maltepe (UCSF) for advice and use of hypoxia chambers.

Competing interests

The authors declare no competing or financial interests.

Author contributions

J.S. conceived of the idea for the study and completed data in Fig. 1, Fig. 4G, Fig. S1A and Fig. S2. M.K.R. completed data in Figs 2, 3, 4A–F. M.Y. and C.S.C. generated microfabricated pillars and analyzed data in Fig. 2E–G. D.L.B. oversaw the project, generated data in Fig. 2A,C, and contributed to data in Fig. S3. All authors contributed to writing the manuscript.

Funding

This work was supported by National Institutes of Health [grant number GM47413 to D.B.]; and the RESBIO Technology Resource for Polymeric Biomaterials (to C.C.). Deposited in PMC for release after 12 months.

Supplementary material

Supplementary material available online at
http://jcs.biologists.org/lookup/suppl/doi:10.1242/jcs.155036/-/DC1

References

Abe, M., Harpel, J. G., Metz, C. N., Nunes, I., Loskutoff, D. J. and Rifkin, D. B. (1994). An assay for transforming growth factor-beta using cells transfected with a plasminogen activator inhibitor-1 promoter-luciferase construct. *Anal. Biochem.* **216**, 276-284.

Boutet, A., De Frutos, C. A., Maxwell, P. H., Mayol, M. J., Romero, J. and Nieto, M. A. (2006). Snail activation disrupts tissue homeostasis and induces fibrosis in the adult kidney. *EMBO J.* **25**, 5603-5613.

Campanholle, G., Ligresti, G., Gharib, S. A. and Duffield, J. S. (2013). Cellular mechanisms of tissue fibrosis. 3. Novel mechanisms of kidney fibrosis. *Am. J. Physiol.* **304**, C591-C603.

Carew, R. M., Wang, B. and Kantharidis, P. (2012). The role of EMT in renal fibrosis. *Cell Tissue Res.* **347**, 103-116.

Chapman, H. A. (2011). Epithelial-mesenchymal interactions in pulmonary fibrosis. *Annu. Rev. Physiol.* **73**, 413-435.

Cowden Dahl, K. D., Robertson, S. E., Weaver, V. M. and Simon, M. C. (2005). Hypoxia-inducible factor regulates alphavbeta3 integrin cell surface expression. *Mol. Biol. Cell* **16**, 1901-1912.

Du, J., Chen, X., Liang, X., Zhang, G., Xu, J., He, L., Zhan, Q., Feng, X. Q., Chien, S. and Yang, C. (2011). Integrin activation and internalization on soft ECM as a mechanism of induction of stem cell differentiation by ECM elasticity. *Proc. Natl. Acad. Sci. USA* **108**, 9466-9471.

Fan, L., Sebe, A., Péterfi, Z., Masszi, A., Thirone, A. C., Rotstein, O. D., Nakano, H., McCulloch, C. A., Szászi, K., Mucsi, I. et al. (2007). Cell contact-dependent regulation of epithelial-myofibroblast transition via the rho-rho kinase-phospho-myosin pathway. *Mol. Biol. Cell* **18**, 1083-1097.

Fu, J., Wang, Y. K., Yang, M. T., Desai, R. A., Yu, X., Liu, Z. and Chen, C. S. (2010). Mechanical regulation of cell function with geometrically modulated elastomeric substrates. *Nat. Methods* **7**, 733-736.

Haase, V. H. (2009). Pathophysiological Consequences of HIF Activation: HIF as a modulator of fibrosis. *Ann. N. Y. Acad. Sci.* **1177**, 57-65.

Haynes, J., Srivastava, J., Madson, N., Wittmann, T. and Barber, D. L. (2011). Dynamic actin remodeling during epithelial-mesenchymal transition depends on increased moesin expression. *Mol. Biol. Cell* **22**, 4750-4764.

Henderson, N. C. and Sheppard, D. (2013). Integrin-mediated regulation of TGFβ in fibrosis. *Biochim. Biophys. Acta* **1832**, 891-896.

Higgins, D. F., Kimura, K., Bernhardt, W. M., Shrimanker, N., Akai, Y., Hohenstein, B., Saito, Y., Johnson, R. S., Kretzler, M., Cohen, C. D. et al. (2007). Hypoxia promotes fibrogenesis in vivo via HIF-1 stimulation of epithelial-to-mesenchymal transition. *J. Clin. Invest.* **117**, 3810-3820.

Hocevar, B. A., Prunier, C. and Howe, P. H. (2005). Disabled-2 (Dab2) mediates transforming growth factor β (TGFbeta)-stimulated fibronectin synthesis through TGFbeta-activated kinase 1 and activation of the JNK pathway. *J. Biol. Chem.* **280**, 25920-25927.

Humphreys, B. D., Lin, S. L., Kobayashi, A., Hudson, T. E., Nowlin, B. T., Bonventre, J. V., Valerius, M. T., McMahon, A. P. and Duffield, J. S. (2010). Fate tracing reveals the pericyte and not epithelial origin of myofibroblasts in kidney fibrosis. *Am. J. Pathol.* **176**, 85-97.

Iwano, M., Plieth, D., Danoff, T. M., Xue, C., Okada, H. and Neilson, E. G. (2002). Evidence that fibroblasts derive from epithelium during tissue fibrosis. *J. Clin. Invest.* **110**, 341-350.

Kalluri, R. and Weinberg, R. A. (2009). The basics of epithelial-mesenchymal transition. *J. Clin. Invest.* **119**, 1420-1428.

Karydis, A., Jimenez-Vidal, M., Denker, S. P. and Barber, D. L. (2009). Mislocalized scaffolding by the Na-H exchanger NHE1 dominantly inhibits fibronectin production and TGF-β activation. *Mol. Biol. Cell* **20**, 2327-2336.

Keely, S., Glover, L. E., MacManus, C. F., Campbell, E. L., Scully, M. M., Furuta, G. T. and Colgan, S. P. (2009). Selective induction of integrin beta1 by hypoxia-inducible factor: implications for wound healing. *FASEB J.* **23**, 1338-1346.

Kim, K. K., Kugler, M. C., Wolters, P. J., Robillard, L., Galvez, M. G., Brumwell, A. N., Sheppard, D. and Chapman, H. A. (2006). Alveolar epithelial cell

mesenchymal transition develops in vivo during pulmonary fibrosis and is regulated by the extracellular matrix. *Proc. Natl. Acad. Sci. USA* **103**, 13180-13185.
Laping, N. J., Grygielko, E., Mathur, A., Butter, S., Bomberger, J., Tweed, C., Martin, W., Fornwald, J., Lehr, R., Harling, J. et al. (2002). Inhibition of transforming growth factor (TGF)-beta1-induced extracellular matrix with a novel inhibitor of the TGF-β type I receptor kinase activity: SB-431542. *Mol. Pharmacol.* **62**, 58-64.
Lee, S. H., Lee, Y. J. and Han, H. J. (2011). Role of hypoxia-induced fibronectin-integrin β1 expression in embryonic stem cell proliferation and migration: Involvement of PI3K/Akt and FAK. *J. Cell. Physiol.* **226**, 484-493.
Leiss, M., Beckmann, K., Girós, A., Costell, M. and Fässler, R. (2008). The role of integrin binding sites in fibronectin matrix assembly in vivo. *Curr. Opin. Cell Biol.* **20**, 502-507.
Leung, K. C., Tonelli, M. and James, M. T. (2013). Chronic kidney disease following acute kidney injury-risk and outcomes. *Nat. Rev. Nephrol.* **9**, 77-85.
Lin, S. L., Kisseleva, T., Brenner, D. A. and Duffield, J. S. (2008). Pericytes and perivascular fibroblasts are the primary source of collagen-producing cells in obstructive fibrosis of the kidney. *Am. J. Pathol.* **173**, 1617-1627.
Liu, Y. (2004). Epithelial to mesenchymal transition in renal fibrogenesis: pathologic significance, molecular mechanism, and therapeutic intervention. *J. Am. Soc. Nephrol.* **15**, 1-12.
McKeown-Longo, P. J. and Mosher, D. F. (1983). Binding of plasma fibronectin to cell layers of human skin fibroblasts. *J. Cell Biol.* **97**, 466-472.
Miettinen, P. J., Ebner, R., Lopez, A. R. and Derynck, R. (1994). TGF-beta induced transdifferentiation of mammary epithelial cells to mesenchymal cells: involvement of type I receptors. *J. Cell Biol.* **127**, 2021-2036.
Nath, B. and Szabo, G. (2012). Hypoxia and hypoxia inducible factors: diverse roles in liver diseases. *Hepatology* **55**, 622-633.
Ni, H., Li, A., Simonsen, N. and Wilkins, J. A. (1998). Integrin activation by dithiothreitol or Mn2+ induces a ligand-occupied conformation and exposure of a novel NH2-terminal regulatory site on the beta1 integrin chain. *J. Biol. Chem.* **273**, 7981-7987.
Noble, P. W., Barkauskas, C. E. and Jiang, D. (2012). Pulmonary fibrosis: patterns and perpetrators. *J. Clin. Invest.* **122**, 2756-2762.
Orphanides, C., Fine, L. G. and Norman, J. T. (1997). Hypoxia stimulates proximal tubular cell matrix production via a TGF-beta1-independent mechanism. *Kidney Int.* **52**, 637-647.
Riedl, J., Crevenna, A. H., Kessenbrock, K., Yu, J. H., Neukirchen, D., Bista, M., Bradke, F., Jenne, D., Holak, T. A., Werb, Z. et al. (2008). Lifeact: a versatile marker to visualize F-actin. *Nat. Methods* **5**, 605-607.
Rock, J. R., Barkauskas, C. E., Cronce, M. J., Xue, Y., Harris, J. R., Liang, J., Noble, P. W. and Hogan, B. L. (2011). Multiple stromal populations contribute to pulmonary fibrosis without evidence for epithelial to mesenchymal transition. *Proc. Natl. Acad. Sci. USA* **108**, E1475-E1483.
Ryu, M. H., Park, H. M., Chung, J., Lee, C. H. and Park, H. R. (2010). Hypoxia-inducible factor-1alpha mediates oral squamous cell carcinoma invasion via upregulation of alpha5 integrin and fibronectin. *Biochem. Biophys. Res. Commun.* **393**, 11-15.
Shin, H. W., Cho, K., Kim, D. W., Han, D. H., Khalmuratova, R., Kim, S. W., Jeon, S. Y., Min, Y. G., Lee, C. H., Rhee, C. S. et al. (2012). Hypoxia-inducible factor 1 mediates nasal polypogenesis by inducing epithelial-to-mesenchymal transition. *Am. J. Respir. Crit. Care Med.* **185**, 944-954.
Singh, P., Carraher, C. and Schwarzbauer, J. E. (2010). Assembly of fibronectin extracellular matrix. *Annu. Rev. Cell Dev. Biol.* **26**, 397-419.
Teng, Y., Zeisberg, M. and Kalluri, R. (2007). Transcriptional regulation of epithelial-mesenchymal transition. *J. Clin. Invest.* **117**, 304-306.
Thiery, J. P., Acloque, H., Huang, R. Y. and Nieto, M. A. (2009). Epithelial-mesenchymal transitions in development and disease. *Cell* **139**, 871-890.
Voelkel, N. F., Mizuno, S. and Bogaard, H. J. (2013). The role of hypoxia in pulmonary vascular diseases: a perspective. *Am. J. Physiol.* **304**, L457-L465.
Yang, M. T., Fu, J., Wang, Y. K., Desai, R. A. and Chen, C. S. (2011). Assaying stem cell mechanobiology on microfabricated elastomeric substrates with geometrically modulated rigidity. *Nat. Protoc.* **6**, 187-213.
Yoneda, A., Ushakov, D., Multhaupt, H. A. B. and Couchman, J. R. (2007). Fibronectin matrix assembly requires distinct contributions from Rho kinases I and -II. *Mol. Biol. Cell* **18**, 66-75.
Zeisberg, M. and Kalluri, R. (2012). Cellular mechanisms of tissue fibrosis. 1. Common and organ-specific mechanisms associated with tissue fibrosis. *Am. J. Physiol. Cell Physiol.* **304**, C216-C225.
Zeisberg, M., Yang, C., Martino, M., Duncan, M. B., Rieder, F., Tanjore, H. and Kalluri, R. (2007). Fibroblasts derive from hepatocytes in liver fibrosis via epithelial to mesenchymal transition. *J. Biol. Chem.* **282**, 23337-23347.